



HAL
open science

Winter temperature conditions (1670–2010) reconstructed from varved sediments, western Canadian High Arctic

Benjamin Amann, Scott F Lamoureux, Maxime P Boreux

► **To cite this version:**

Benjamin Amann, Scott F Lamoureux, Maxime P Boreux. Winter temperature conditions (1670–2010) reconstructed from varved sediments, western Canadian High Arctic. *Quaternary Science Reviews*, 2017, 172, pp.1 - 14. 10.1016/j.quascirev.2017.07.013 . hal-04276260

HAL Id: hal-04276260

<https://hal.science/hal-04276260>

Submitted on 14 Dec 2023

HAL is a multi-disciplinary open access archive for the deposit and dissemination of scientific research documents, whether they are published or not. The documents may come from teaching and research institutions in France or abroad, or from public or private research centers.

L'archive ouverte pluridisciplinaire **HAL**, est destinée au dépôt et à la diffusion de documents scientifiques de niveau recherche, publiés ou non, émanant des établissements d'enseignement et de recherche français ou étrangers, des laboratoires publics ou privés.

1 **Winter temperature conditions (1670 – 2010) reconstructed from varved**
2 **sediments, western Canadian High Arctic**

3 Amann Benjamin ⁽¹⁾, Lamoureux Scott F. ⁽¹⁾, Boreux Maxime P. ⁽¹⁾

4 ⁽¹⁾ Department of Geography and Planning, Queen's University, Kingston, ON, K7L 3N6
5 (Canada)

6 benjamin.amann@queensu.ca

7

8

9 **Keywords:**

10 Lake sediments – Snow melt – Winter climate – Climate change – Sedimentology –
11 Paleoclimatology

12

13 **Highlights:**

- 14 1. The nival sedimentary units of the varves are isolated from the rainfall units
15 2. The thickness of the nival units is used to predict NDJFM temperature and
16 snowfall
17 3. Winter NDJFM reconstruction is valid for a large part of the Canadian Arctic
18 4. This winter record captures most of the annual climate variability back to CE
19 1670

20 **Abstract**

21

22 Advances in paleoclimatology from the Arctic have provided insights into long-term
23 climate conditions. However, while past annual and summer temperature have received
24 considerable research attention, comparatively little is known about winter
25 paleoclimate. Arctic winter is of special interest as it is the season with the highest
26 sensitivity to climate change, and because it differs substantially from summer and
27 annual measures. Therefore, information about past changes in winter climate is key to
28 improve our knowledge of past forced climate variability and to reduce uncertainty in
29 climate projections. In this context, Arctic lakes with snowmelt-fed catchments are
30 excellent potential winter climate archives. They respond strongly to snowmelt-induced
31 runoff, and indirectly to winter temperature and snowfall conditions. To date, only a few
32 well-calibrated lake sediment records exist, which appear to reflect site-specific
33 responses with differing reconstructions. This limits the possibility to resolve large-scale
34 winter climate change prior the instrumental period.

35 Here, we present a well-calibrated quantitative temperature and snowfall record for the
36 extended winter season (November through March; NDJFM) from Chevalier Bay
37 (Melville Island, NWT, Canadian Arctic) back to CE 1670. The coastal embayment has a
38 large catchment influenced by nival terrestrial processes, which leads to high
39 sedimentation rates and annual sedimentary structures (varves). Using detailed
40 microstratigraphic analysis from two sediment cores and supported by μ -XRF data, we
41 separated the nival sedimentary units (spring snowmelt) from the rainfall units
42 (summer) and identified subaqueous slumps. Statistical correlation analysis between
43 the proxy data and monthly climate variables reveals that the thickness of the nival units
44 can be used to predict winter temperature ($r= 0.71$, $p_c < 0.01$, 5-yr filter) and snowfall ($r=$
45 0.65 , $p_c < 0.01$, 5-yr filter) for the western Canadian High Arctic over the last ca. 400
46 years. Results reveal a strong variability in winter temperature back to CE 1670 with the
47 coldest decades reconstructed for the period CE 1800-1880, while the warmest decades
48 and major trends reconstructed for the period CE 1880-1930 ($0.26^\circ\text{C}/\text{decade}$) and CE
49 1970-2010 ($0.37^\circ\text{C}/\text{decade}$). Although the first aim of this study was to increase the
50 paleoclimate data coverage for the winter season, the record from Chevalier Bay also

51 holds great potential for more applied climate research such as data-model comparisons
52 and proxy-data assimilation in climate model simulations.

53 **1 Introduction**

54

55 The Arctic is recognized as one of the most sensitive regions to climate change (ACIA
56 2004; Collins et al. 2013). Amplified warming of the Arctic climate has long been
57 demonstrated from both observations and simulations (Hardy et al. 1996; Moritz et al.
58 2002; Miller et al. 2010; Comiso and Hall, 2014). This warming has led to increases in
59 high-latitude precipitation that are particularly notable during the winter season
60 (Kattsov and Walsh, 2000; Bintanja and Selten, 2014).

61 Arctic warming has been considered unprecedented over the past thousand years based
62 on available paleoclimate data. Information about past climate variability is essential to
63 assess the sensitivity of the Earth's climate to natural and anthropogenic forcings, and to
64 reduce uncertainty in future climate projections (Masson-Delmotte et al. 2013). For the
65 Arctic, the most comprehensive studies of climate change assessment covered the past
66 four centuries (Overpeck et al. 1997), the last two millennia (Kaufman 2009; McKay and
67 Kaufman 2014), and the Holocene (Sundqvist et al. 2014; Briner et al. 2016).

68 However, while most of the paleoclimate records in the Arctic are related to annual and
69 summer temperature (Briner et al. 2016), comparatively little has been reported about
70 winter paleoclimate (e.g. Cuvén et al. 2011). As an example, only four winter
71 reconstructions out of over fifty-six records were considered in the extended database
72 used to reconstruct Arctic temperatures by McKay and Kaufman (2014). As a result,
73 seasonality is hardly considered in climate models, especially regarding the winter
74 season (Goosse et al. 2010). Winter climate is of particular interest because it is the
75 season with the highest sensitivity to climate change (Thompson and Wallace, 1998;
76 Rinke et al. 1999; Moritz et al. 2002), which greatly differs from summer and annual
77 measures (Jones et al. 2014). Therefore, information about past changes in winter
78 climate is required in order to reduce uncertainty in large-scale assessments of climate
79 variability and change.

80 In this context, Arctic lakes and similar sedimentary settings are excellent potential
81 climate archives owing to their capacity to preserve climate variability through very
82 long times and at a high temporal resolution (Hughen et al. 1996). Moreover, these
83 Arctic environments provide very specific and advantageous settings such as a strong
84 sensitivity to extreme seasonal variations in processes (stream flow and sediment

85 delivery), and limited direct human impact (Smol and Douglas, 1996; Lamoureux and
86 Gilbert, 2004). In particular, Arctic lakes with nival catchments were shown to respond
87 directly to the length and the intensity of the snowmelt, and indirectly to winter
88 temperature and snowfall conditions on the previous year (Forbes and Lamoureux
89 2005; Cockburn and Lamoureux, 2008).

90 Nevertheless, reconstructing past climate from Arctic lakes remains an analytical
91 challenge. For instance, low ^{210}Pb inventories and the paucity of degradable-terrestrial
92 remains limit ^{210}Pb and ^{14}C dating, respectively (Wolfe et al. 2004). Moreover, low
93 sedimentation accumulation rates in some Arctic lakes may restrict the temporal
94 resolution and the length of the paleoclimate records. This is the reason why annually
95 laminated sediments (varves) have received a growing scientific attention over the past
96 two decades. Varved sediments are recognised as a useful tool for Arctic
97 paleoclimatology (Hughen et al. 1996), which have provided successful paleoclimate
98 examples from the Canadian High Arctic (Wolf and Smith, 2004; Besonen et al. 2008).

99 To date, only a few annually-resolved and well-calibrated sediment records exist for the
100 winter season (e.g. Cuven et al. 2011). Moreover, results from individual records suggest
101 a strong sensitivity to: (i) local changes in winter climate; and (ii) specific catchment
102 properties and snowmelt response. This local focus has resulted in a great diversity
103 among the records, with typical examples such as: June temperature (Hughen et al.
104 2000), August-to-October temperature and snowfall (Tomkins et al. 2010), snowmelt
105 intensity (Francus et al. 2002), and September-to-May temperature and May snow depth
106 (Cuven et al. 2011). These differences in the records clearly limit the possibility to
107 resolve large-scale and regional patterns of winter climate change prior the
108 instrumental period.

109 Here, we present a well-calibrated quantitative temperature record for the extended
110 winter season (November through March; NDJFM), which is representative of a large
111 part of the Canadian High Arctic. Using detailed microstratigraphical analysis supported
112 by an annual chronology, we demonstrate that the relatively thick varves from Chevalier
113 Bay (Melville Island, NWT) contain a winter temperature signal, which can be
114 reconstructed for the past ca. 400 years. With this paleoclimate record, we demonstrate
115 that the indirect information stored in the winter temperature and snowfall conditions
116 holds great potential for more advanced application in climate research.

117 2 Study site

118

119 Chevalier Bay (75°03'10"N, 111°30'38"W; unofficial name) is a coastal marine setting
120 located on Melville Island, Dundas Peninsula, Northwest Territories in the Canadian
121 High Arctic. The bay is located about 50 km west from the Cape Bounty Arctic
122 Watershed Observatory (CBAWO; Fig. 1a); a research site where hydrological, sediment
123 transport and lake deposition studies have been undertaken since 2003. Chevalier Bay is
124 a small marine embayment that is largely isolated from the ocean and marked by a
125 sedimentary environment similar to a coastal lacustrine basin. The catchment is strongly
126 influenced by terrestrial processes and can be regarded as a nival catchment (Cockburn
127 and Lamoureux, 2008), enabling the sediment record from Chevalier Bay to be
128 compared with other Arctic nival-lake sediment records. Of particular interest, its
129 catchment has a remarkably large area (350 km²); 152 times larger than the area of the
130 bay (Fig. 1b). This catchment feature leads to high sedimentation rates (mean 2.53 mm
131 yr⁻¹), atypical of other studied Arctic sites (common annual rates range from 0.2 to 1
132 mm; e.g. Tomkins et al. 2010; Francus et al. 2002, respectively).

133 The bedrock of the area consists of folded Devonian iron-rich weathered sandstone and
134 siltstone (Hodgson et al. 1984; Christie and McMillan, 1994). The landscape features a
135 limited relief (max. 110 m a.s.l.) with the drainage system developing on sparse tundra
136 vegetation and continuous permafrost (Fig. 1b).

137 The climate of the region is classified as polar desert (tundra climate *ETf*; Köppen-Geiger
138 classification) characterized by cold winters, cool summers, and limited annual
139 precipitation that falls primarily as snow during the autumn/winter season (Fig. 1c).
140 Mean summer (JJA) and extended winter (NDJFM) temperatures are 3.5°C and -27.8°C,
141 respectively (CE 1949 – 1997; Mould Bay meteorological station, 280km to the west;
142 Figure 1). Annual precipitation is dominated by winter snowfall leading to a maximum
143 mean snow accumulation of 300 mm depth in early May, while rare high-intensity
144 rainfall events (> 10 mm/day) occur in summer (Fig. 1c). Total annual precipitation
145 amounts to 98 mm.

146 Chevalier Bay is at sea level and connected to the Arctic Ocean by an estimated 7-m deep
147 narrow inlet, enabling tidal interaction during the short ice-free period (July-August to
148 early October). Properties of the 16-m deep water-column of Chevalier Bay were

149 measured in June 2010 (Fig 2). It reveals two chemoclines at 3 and 7 m depth, with the
150 hypolimnion characterised by quasi-anoxic conditions (<10 % saturation) and saline
151 water of 35 PSU. In spring, snowmelt-induced freshwater enters the lake under the ice
152 cover (~2-m thick), which is marked by low salinity (4 PSU), a peak in turbidity (58
153 NTU), warmer temperature (1°C), and high dissolved oxygen content (85% saturation).

154

155

156 **3 Material and methods**

157

158 The study of snowmelt-induced processes and the relationship between stream
159 discharge and suspended sediment transport could not be conducted at Chevalier Bay.
160 However, such research was undertaken at nearby West and East Lakes in CBAWO (Fig.
161 1a), and will be used for comparison and correlation. This nearby site has similar
162 hydroclimate, topography, surface materials, vegetation and geology (Cockburn and
163 Lamoureux, 2008; Lewis et al., 2012).

164

165

166 **3.1 Sediment coring and processing**

167

168 Two sediment cores were retrieved from Chevalier Bay in June 2010 with a Universal
169 gravity-percussion corer (Aquatic Research Instruments); one from the middle (10CV03,
170 86cm long), and another from a more proximal location (10CV04, 46cm long) (Fig. 1b).
171 The comparison between these two cores was used to: (i) identify anomalous deposits;
172 and (ii) assess whether varve thickness could be consistently used as a proxy through
173 non-localized differences in sedimentation rates (Fig. S1; Tomkins et al. 2010). Cores
174 were transported and stored unfrozen to the laboratory. Only data from core 10CV03
175 are shown here, which offer the longest record.

176 In the laboratory, the cores were split lengthwise and photographed prior to analysis.
177 Non-destructive X-Ray Fluorescence (XRF) scans were obtained on the first core half
178 (60kV, 160 mA, and 80 ms exposure time) at INRS Québec. XRF elements were selected

179 following Croudace et al. (2006) and Kylander et al. (2011), with a special focus on the
180 ratios Zr/K and Fe/Rb . These two XRF ratios were successfully applied to estimate grain
181 size variability in sediment cores from East Lake (Cape Bounty, Melville Island, 50 km
182 east); a site with bedrock and sedimentary setting comparable to Chevalier Bay (Cuven
183 et al. 2010, 2011; Lapointe et al. 2012).

184

185 3.2 Thin sections: microstratigraphy and sediment chronology

186

187 Micro-stratigraphical analysis of the varves and the sediment chronology were
188 generated from merged optical microscopy thin section images (resolution= 0.02 mm;
189 magnification x10). Thin sections were prepared from overlapping sediment slabs (7 x 2
190 x 1 cm) and dehydrated with acetone prior to embedding with Spurr's epoxy resin
191 (Lamoureux 1994). Two analysts (BA and MB) independently counted the laminae
192 seven months apart and manually measured the thickness of each specific sedimentary
193 unit (nival, rainfall, and clay cap). The graphic software CorelDraw (0.05-mm resolution)
194 was used to delineate sedimentary units from scanned images. Counting uncertainty
195 was derived from the standard deviation of the independent chronologies.

196 To validate the varve hypothesis (annual character of the layers), 33 samples were
197 extracted from core 10CV03 with depth intervals of 0.5 to 1.0 cm for radioisotope dating
198 (Wolf et al. 2004). Samples were analysed for ^{210}Pb and ^{137}Cs using the gamma-ray
199 spectrometry facilities (EGG-Ortec type spectrometer, well germanium detector,
200 capacity 10 cm³) at the PEARL Laboratory (Queen's University, Kingston, ON, Canada).

201

202 3.3 Climate data and proxy-climate calibration

203

204 Monthly climate data were obtained from local and more distant meteorological stations
205 to cover a broad geographical representativeness of the climate variability in the region
206 (Fig. 1a). Local data for the CBAWO meteorological station were accessed from Polar
207 Data Catalogue (www.polardata.ca; 2003-2015 Climate Data Station, Cape Bounty,
208 Nunavut; CCIN Ref No: 9885; 74.9N/-109.5E). Longer instrumental climate data were

209 accessed from Environment Canada (www.climat.meteo.gc.ca) for the selected stations
210 of Mould Bay A (CE 1949-1997) and Resolute CARS (CE 1947-2015). Note that Mould
211 Bay measurements were discontinued in 1997 and restarted in 2002 with an automatic
212 station at a different location. We have no means of determining the potential difference
213 between the earlier and later data sets, and hence, we conservatively do not extend the
214 Mould Bay station series after 1997. We also selected the gridded data of observed
215 climate CRU TS 3.23 centered on our study site (Harris et al., 2014; 0.5° resolution), for
216 the calibration with the proxy dataset (CE 1949-2015, grid cell: 11.75-11.25° W; 64.75-
217 75.25° N).

218 To test the sensitivity of Chevalier Bay to climate variability, varve thickness for each
219 seasonal phase was correlated with individual monthly data and 2-to-12-month
220 windows for temperature (mean) and precipitation (cumulative rainfall and snowfall)
221 from all meteorological stations and the gridded dataset (multiple testing; de Jong and
222 Kamenik, 2011). Both the proxy and the climate data were presented with a 5-year
223 triangular filter prior to calibration, to account for: (i) dating uncertainty from the
224 different varve counts; and (ii) error introduced by sediment sampling. Accordingly, the
225 probability values (p) were corrected for serial autocorrelation (p_c). The best correlation
226 from this multiple testing was then used to develop a proxy-climate calibration model,
227 using an Ordinary Least-Squares (OLS) regression model (inverse regression), following
228 the calibration-in-time approach (CIT) described by von Gunten et al. (2012). To
229 validate the model, the root mean squared error of prediction (RMSEP) inferred from
230 the bootstrap cross-validation method was preferred to the split period approach, due
231 to a change in the variance post CE 1900 (Birks 2005; Amann et al. 2015). Finally, this
232 model was used to reconstruct climate variability for the length of the chronology.

233 4 Results

234

235 4.1 Sediment properties and varve characterization

236

237 Sediments recovered from both locations of Chevalier Bay consist mainly of light- to
238 dark-grey (Munsell colour: 2.5Y-6/1 to 2.5Y-4/1, respectively) laminated clastic
239 material (Fig. 3a). Two primary sedimentary units occur throughout the sediment
240 sequence with: (i) sedimentary couplets interpreted as clastic varves (mean thickness =
241 2.53 mm); and (ii) thick and coarser-grain deposits interpreted as turbidites. Turbidite
242 layers are characterized by much higher sedimentation rates in the proximal core
243 (10CV04, >0.9 cm) compared to the more central site (10CV03, >0.6 cm; Fig. 1b). On the
244 contrary, laminae interpreted as varves have comparable sedimentation rates at the two
245 locations (core-to-core layer-thickness comparison; $R^2= 0.879$ comprising all layers
246 compared with $R^2= 0.928$ without turbidites).

247 Fig. 3b shows a typical varve structure that comprises: (i) a light-grey coarse-silt spring
248 deposit characterized by rather high Zr/K values (spring snowmelt = nival unit); (ii) a
249 dark-grey/black coarse-silt to fine-sand deposit characterized by high Zr/K values
250 (summer rainfall = rainfall unit); and (iii) an oxidized clay cap marked by the highest
251 Fe/Rb and the lowest Zr/K values. Six varve facies types were derived from detailed
252 stratigraphic analysis of the thin sections (Fig. 4).

- 253 • Facies type 1: simple couplets compose the varve, with a snowmelt-induced
254 deposit (hereafter defined as nival unit) and a winter oxidized clay cap.
- 255 • Facies type 2: a rainfall unit characterised by coarser particles and organic
256 remains is found on top of the nival unit.
- 257 • Facies type 3: the rainfall unit is intercalated between two nival units, most likely
258 due to early-season rainfall events.
- 259 • Facies type 4: anomalously thick nival units (up to 8 mm. yr⁻¹) characterize this
260 facies type, which is found at a core depth of 20-30 cm mainly (2.9% occurrence).
- 261 • Facies type 5: non-oxidized clay deposits are intercalated between nival units,
262 most likely due to extended periods of calm conditions within the snowmelt
263 season.

- 264 • Facies type 6: coarse-grained deposits are randomly intercalated within the
265 varves, interpreted as slumps triggered by internal basin processes.

266 Although the nival unit and the clay cap are found each year (100% occurrence), the
267 rainfall unit occurring in Facies type 2 and type 3 is only found in 141 of the 343 layers
268 (41.1% occurrence).

269

270 4.2 Age-depth modelling

271

272 The chronology built from the different lamina counts is consistent with the ^{137}Cs dating
273 technique, which supports the varve hypothesis (Fig. 5). The ^{137}Cs profile shows a peak
274 at a 14-cm depth (2.74 ± 0.23 dpm g^{-1}) and drops to 0 level values below 17 cm.
275 Estimated varve ages for these two depths are 1961 ± 2 yrs (bomb testing peak) and
276 1952 ± 3 yrs (onset of ^{137}Cs deposition), respectively.

277 The counting uncertainty shows a maximum of 1.5 % within the instrumental period (CE
278 1948 – 2010), but reaches 6 % at the lowermost section of the sediment core, as
279 reported on the lower panel of Fig. 5. The greatest increases in the counting error occur
280 during the periods CE 1850 – 1825 (1 to 2.7 % counting error, respectively), and CE
281 1750 – 1725 (2.7 to 5.2 %, respectively), indicative of sediment sections with varves that
282 are less well preserved.

283

284 4.3 Proxy-climate calibration and validation

285

286 On the basis of this sedimentological analysis together with knowledge about the
287 regional hydroclimate, we hypothesize that the thickness of the snowmelt-induced
288 deposit from Chevalier Bay sediments is primarily controlled by the snowmelt
289 conditions (intensity and duration), and by previous winter conditions indirectly
290 (snowfall, snow depth, and temperature).

291 Statistical analysis between sediment proxy and climate data reveals that the thickness
292 of the nival units contains a winter temperature signal, with the best correlation found
293 for the extended winter season; November through March (NDJFM). This result is

294 consistent among all meteorological stations and gridded data with: $r = 0.71$ ($p_c < 0.01$, $n =$
295 59 , 5-yr filtered) for CRU TS, $r = 0.66$ ($p_c < 0.01$, $n = 46$, 5-yr filtered) for Mould Bay, and $r =$
296 0.65 ($p_c < 0.01$, $n = 59$, 5-yr filtered) for Resolute Bay (Fig. 6, Table 1). Significant negative
297 correlation is also consistently found between the thickness of the nival units and
298 August-through-October (ASO) temperature. The PCA biplot illustrates these
299 correlation results through the position of the ASO vector aligned with the varve proxy
300 (nival unit), but in the opposite direction (Fig. 6). On the contrary, no significant
301 correlation can be found for summer (JJA) and autumn (SON) temperatures that are
302 associated with eigenvectors positioned orthogonally to the varve proxy. Spring
303 temperature data (MAM) forms an independent cluster, and is not significantly
304 correlated with the thickness of the nival units (Table 1). Statistical tests also revealed
305 positive correlations with winter NDJFM precipitation and snowfall, which are
306 significant for Resolute and CRU TS but not for Mould Bay (Table 1).

307 Based on these results from multiple testing, a calibration-in-time model was developed
308 between the thickness of the nival unit and NDJFM temperature from CRU TS (Fig. 7a).
309 The performance of this model is given by the following parameters: $r = 0.71$, $n = 59$, $p_c <$
310 0.01 , RMSEP = 0.65°C that corresponds to 19.9% of the peak to peak amplitude and 2.0%
311 of the mean. Although Mould Bay best represents the climate conditions on Melville
312 Island (daily data; Mould Bay vs. CBAWO, $R^2 = 0.97$, $n = 2537$, data not shown), the Mould
313 Bay record limits the calibration period to CE 1948 – 1997. Therefore, the gridded data
314 from CRU TS 3.23 was preferred, extending the period to CE 2010. The Resolute Bay
315 station records similar long-term temperature variability (Resolute vs. CRU TS; $R^2 =$
316 0.83), but shows much warmer conditions (Fig. 7).

317

318 4.4 Climate reconstruction

319

320 Based on the calibration-in-time model, the thickness of the nival units was used to
321 reconstruct NDJFM temperature from Chevalier Bay back to CE 1670 (Fig. 8a). The
322 record shows pronounced sub- and multi-decadal variability, which remains well within
323 the calibration range apart from 11 years of the warm period CE 1920-1940. Relatively
324 cold winters occur from CE 1670 to CE 1800 with mean NDJFM temperature of -32.2°C .

325 This mean value drops to -32.7°C for the period CE 1800-1880; the coldest decades over
326 the past ca. 350 years. Finally, two major warming trends are estimated in the 20th-21st
327 centuries for the periods CE 1880-1930 and CE 1970-2010. They are marked by rates of
328 0.26°C and 0.37°C per decade, respectively.

329 The quantitative winter temperature reconstruction from Chevalier Bay is
330 representative of a large part of the western Canadian High Arctic (Fig. 8). The
331 correlation map for the NDJFM season reveals a signal extending from the south of
332 Victoria Island to the northernmost point of Ellesmere Island, and eastward (although
333 diminishing in strength) to north-western Greenland (Fig. 8b). Our reconstruction is also
334 consistent with other temperature records from this part of the Arctic (Fig. 8a).
335 Significant correlation is found between the Chevalier Bay record and temperature-
336 driven changes in mass balance of South Melville and Devon Ice Caps ($r= 0.37$, $p< 0.01$,
337 $n= 385$; Fisher et al. 1983; Boon et al. 2010). Additionally, multi-decadal changes of the
338 NDJFM record (31-yr filtered) agree well with annual temperature anomaly for the
339 entire Arctic region north of 60°N (Fig. 8a).

340 **5 Discussion**

341

342 5.1 Sedimentology and varve stratigraphy

343

344 The clastic varve interpretation was based on the strong seasonality of hydroclimate in
345 the region. Hydrological runoff generally occurs over 3 to 4 months per year from June
346 to August/September (Cockburn and Lamoureux, 2008), leading to sustained material
347 delivery from surficial sediments and poorly consolidated bedrock (Favaro and
348 Lamoureux, 2014). In winter, persistent ice cover preserves the primary structure of the
349 sediments in this relatively deep basin and fluvial activity ceases.

350 The sediments of Chevalier Bay exhibit abnormally thick varves owing to its large
351 catchment size (Fig. 1b). Indeed, the varves found in the bay (mean thickness of 2.53
352 mm) are thicker than what is commonly reported by studies on nival Arctic lakes.
353 Among others, mean annual thickness of ~0.2 mm was reported from Lake A (Tomkins
354 et al. 2010), ~0.75 mm from Sanagak Lake (Lamoureux 2006), ~0.8 mm in East Lake
355 (Cuven et al. 2011), and up to 1 mm in Sawtooth Lake (Francus et al. 2002). High annual
356 sedimentation rates from Chevalier Bay enabled us to identify and separate the different
357 sedimentation processes through the entire sediment sequence.

358 Using detailed stratigraphical analysis (Fig. 3, Fig. 4), the nival units (spring snowmelt)
359 could be clearly distinguished from the rainfall units (summer), from slumps and clay
360 caps (winter). This classification was the cornerstone for the development of: (i) a
361 reliable and precise chronology; and (ii) a good proxy-climate calibration model. In
362 particular, different facies types of varves could be identified based on the absence
363 (facies 1) and the timing of the rainfall unit (facies 2 and 3), the thickness of the nival
364 unit (facies 4), and its internal structure (facies 5). In this exercise, Zr/K ratios from XRF
365 scans were particularly supportive as a visual indicator of particle size, reproducing the
366 sedimentary interpretation model developed by Cuven et al. (2010, 2011) and Lapointe
367 et al. (2012) from East Lake, 50 km away.

368 Interestingly, the nival unit appeared as the primary sediment deposition unit compared
369 to thinner (average 0.96 mm) and uncommon rainfall events (41 % of years). These
370 small deposits were most likely buffered by the large catchment size and the low relief

371 of the catchment, and/or dampened by antecedent conditions. This pattern is consistent
372 with numerous studies from nival lakes in the Arctic, which showed that most of the
373 total sediment transport occurs with the onset of snowmelt (Hardy et al. 1996; Braun et
374 al. 2000; Forbes and Lamoureux, 2005; Cockburn and Lamoureux, 2008; Tomkins et al.
375 2010).

376 Varves are known to integrate multiple and complex catchment and lake processes,
377 which can mask the nival signal (Hambley and Lamoureux, 2006). In a similar study,
378 Francus et al. (2008) combined detailed sedimentological analysis and limno-
379 hydroclimatical observations from Sawtooth Lake to disregard varve thickness as a
380 valuable climate proxy on its own. Also, several studies from Arctic lakes have
381 demonstrated the advantage of thicker varves in: (i) differentiating processes that lead
382 to the formation of varves; and (ii) highlighting the prime role of nival runoff. This was
383 the case for Nicolay Lake (Cornwall Island; Lamoureux 2000; Hambley and Lamoureux,
384 2006), Bear Lake (Devon Island; Lamoureux et al. 2002; Lamoureux and Gilbert, 2004)
385 and Lake R (Devon Island; Chutko and Lamoureux, 2008).

386

387 5.2 Varve chronology

388

389 Stratigraphical analysis of the thin sections supported by XRF data was used to develop
390 a precise and reliable varve chronology from Chevalier Bay sediments, back to CE 1670
391 (Fig. 5). Especially, the peak of Fe/Rb in the oxidized clay cap was found to be a
392 consistent marker for the termination of a varve year (Fig. 3, Fig. 4). Iron content
393 associated with the salinity of the hypolimnion of Chevalier Bay (Fig. 2) played a major
394 role in the counting of the varves. The metal, chemically weathered from the iron-rich
395 catchment, is delivered into the Bay by spring (snowmelt) and summer (rainfall) runoff,
396 mainly. Great proportions of highly reactive ferrous iron are present in this saline water,
397 and are then likely to precipitate as ferric hydroxide and to fix to clays (Coey et al. 1974).
398 Finally, modest oxidizing conditions at the sediment-water interface, such as in
399 Chevalier Bay, are sufficient for the formation of iron-rich clay sediments (Haese, 2006).
400 Additionally, the water column properties from Chevalier Bay suggest that the
401 sediments are distributed from the river as overflows across the lake, while underflows
402 are likely discouraged by chemical stratification (Fig. 2).

403 The varve chronology was validated by independent ^{137}Cs chronomarkers, which
404 captured the known Northern Hemisphere peak of nuclear activity in CE 1963 and the
405 onset of cesium deposition in CE 1954 (Fig. 5). Although no geographical consistency
406 could be derived, cesium counts from Chevalier Bay (peak value of 2.7 dpm g^{-1}) were in
407 the same order of magnitude than other Arctic lake studies. For instance, 0.7 dpm g^{-1}
408 were measured at Upper Soper Lake (Baffin Island; Hughen et al. 2000), 7.5 dpm g^{-1} in
409 Nicolay Lake (Cornwall Island; Lamoureux 1999), 9.6 dpm g^{-1} in East Lake (Melville
410 Island; Coven et al. 2011), and 9.7 dpm g^{-1} in Skardtjørna (Svalbard archipelago;
411 Holmgren et al. 2009). In contrast, a consistent and interpretable ^{210}Pb profile could not
412 be developed for our study due to very low lead fallout counts (^{210}Pb excess) in the
413 sediment samples. In a review study, Wolfe et al. (2004) described the influence of
414 developing permafrost and the short ice-free season, which both restrain the transfer of
415 atmospheric ^{210}Pb to the sediments of High Arctic lakes.

416

417 5.3 Winter climate signal: correlations and mechanism

418

419 The proxy-climate correlations revealed the thickness of the varve nival units as a proxy
420 for winter climate conditions of the Canadian High Arctic (Fig. 6 and 7; Table 1). The
421 highest positive correlations were found with CRU TS for NDJFM temperature ($r= 0.71$,
422 $p_c < 0.01$) and NDJFM snowfall ($r= 0.65$, $p_c < 0.01$), while significant negative correlations
423 for ASO temperature on the previous year were found ($r= -0.47$, $p_c < 0.01$). Covariance
424 between these three variables suggests a strong mechanistic relation between winter
425 temperature and snowfall, and subsequent sediment transport and deposition in the Bay.

426 Warm winters associated with increased winter snowfall and snow water equivalent
427 (SWE) are likely to lead to greater snowmelt runoff in spring, and ultimately to higher
428 spring sedimentation rates (*i.e.* thicker nival units). This control of winter conditions
429 over sediment transport through SWE in Chevalier Bay is in close agreement with
430 studies on sediment process understanding from nival watersheds at Cape Bounty and
431 the Boothia Peninsula (Cockburn and Lamoureux 2008; Forbes and Lamoureux 2005;
432 respectively). Additionally, the negative correlations with autumn ASO temperature
433 could be explained by greater rain/snow ratios during warmer autumn seasons,
434 resulting in thinner nival units the following year (distinct from the rainfall units).

435 Moreover, the reliability of these results is strengthened by the consistency among the
436 three climate datasets considered in this study (Mould Bay, Resolute Bay, and CRU TS;
437 Table 1).

438 Although the sources of moisture during winter remains under debate, the link between
439 temperature and precipitation is broadly recognized for the Arctic. The longest available
440 record from Resolute Bay reports significant correlation between NDJFM temperature
441 and NDJFM precipitation ($r= 0.57$, $p< 0.01$, $n= 62$, 5-yr filtered), comparable to the
442 spatial correlations over the Canadian Arctic (Fig. S2). Also, Lafrenière et al. (2013)
443 demonstrated the importance of daily incursion of warm air in winter (with up to 9°C)
444 to the onset of snow cover on Melville Island. Most of the observed 20th- and modelled
445 21st-century increase of Arctic precipitation has been attributed to the variations of the
446 sea surface temperature, especially in late autumn and winter. Sea-ice boundary
447 conditions are considered a major contributor to the total evaporative response in the
448 Arctic, where the sensible-heat transfer between the warm ocean and the cold
449 atmosphere develops even during cold winters (Kattsov and Walsh, 2000; Hall 2004;
450 Kattsov et al. 2007). This is consistent with global climate models that indicate local
451 evaporation changes as the main source of moisture in the Arctic winter (Bintanja and
452 Selten, 2014). Nevertheless, these results contrast with stable water isotopes used as
453 moisture source tracers, which suggest a greater contribution of moisture transport
454 from lower latitudes towards the end of the winter season (Kurita, 2011). This switch
455 from local to more distant moisture origin in winter might in part explain why weaker
456 correlations were found with winter precipitation than with winter temperature in
457 Chevalier Bay. Another part of the explanation remains in the difficulty to measure
458 winter precipitation accurately, especially with subsequent snow redistribution by the
459 wind.

460 Although correlation tests support this mechanistic relation between temperature and
461 precipitation (snowfall) for the winter season, hydroclimate data for the Arctic region
462 should be considered with care. Indeed, precipitation is remarkably heterogeneous in
463 the Arctic, and instrumental observations remain very sparse (Kattsov et al. 2007). This
464 heterogeneity was evidenced by the lower correlations for Mould Bay precipitation and
465 snowfall data, as compared to Resolute and CRU TS (Table 1). Moreover, NDJFM
466 temperature and NDJFM precipitation correlate significantly for Resolute ($r= 0.57$, $p<$

467 0.01, $n=62$), while a weaker and non-significant correlation is recorded from Mould Bay
468 ($r=0.22$, $p>0.05$, $n=40$). Also, Cockburn and Lamoureux (2008) and Cuven et al. (2011)
469 identified this weak spatial consistency between Mould Bay and Resolute for
470 precipitation. The scarcity of high-quality hydroclimate data in the Arctic remains an
471 important limitation, to the extent that it is still regarded as key knowledge gap by the
472 paleoclimate community (Hormes and Bakke, 2014; Hormes et al. 2015).

473 In this context, the best correlation between the thickness of the nival units and NDJFM
474 temperature was used to develop the proxy-climate calibration model (Fig. 7). We
475 rationalize this approach, as many applications in climate research require time series of
476 a single variable and for a specific season of the year, which is typical of data–data
477 comparisons, data-model comparisons or proxy-data assimilation in climate model
478 simulations (Goosse et al. 2010). Two meteorological stations and CRU TS gridded data
479 were used to develop this linear model. This approach strengthens the reproducibility,
480 reliability and spatial representativeness of the climate signal, and differs from the
481 common practice of considering the closest station (e.g. Alert for Lake A, Tomkins et al.
482 2010; Eureka for Sawtooth Lake, Francus et al. 2008; Alert for Lower Lake Murray, Cook
483 et al. 2008; Taloyoak for Sanagak Lake, Lamoureux et al. 2006; Kimmirut for Upper
484 Soper Lake, Hughen et al. 2000). CRU TS 3.23 was particularly effective, providing a
485 continuous and representative record for winter climate conditions at our study site,
486 and with the longest dataset (calibration period CE 1948-2010).

487

488 5.4 Climate reconstruction and regional representativeness

489

490 The varves of Chevalier Bay provide a well-calibrated quantitative winter-temperature
491 record from the Canadian High Arctic, covering the past ca. 400 years (Fig. 8a). Results
492 reveal a strong variability in winter temperature back to CE 1670. The coldest decades
493 are reconstructed for the period CE 1800-1880, while the warmest and most prominent
494 features of the record are reconstructed for the period CE 1880-1930 and CE 1970-2010.
495 The reconstruction provides quantitative temperature estimates for all but the period
496 CE 1920-1940, with values extrapolated outside the range of the calibration period.
497 Although interpreted qualitatively, these two decades are well known to be among the
498 warmest over the past centuries, especially in the Arctic. This warming has been

499 attributed to a combination of internal-natural and external-forced climate variability
500 (Bengtsson et al. 2004; Yamanouchi 2011; Johannessen et al. 2016). However, without
501 validation from other paleoclimate records that this period can be interpreted as an
502 anomalously warm winter period, potential other non-climatic factors might have
503 induced thick nival deposits during this period. Indeed, sedimentary analysis evidences
504 a significant change in varve deposition during this warm period, which might be
505 attributed to different mechanisms such as: (i) a change in the sediment trajectory
506 through temporary delta channel avulsion; (ii) the hydrological influence of antecedent
507 soil moistening during these warm and wet decades; (iii) a change of sediment
508 availability in the catchment; and/or (iv) the occurrence of gullies in the bathymetry of
509 Chevalier Bay (turbidity current pathways). Although further work would be required to
510 resolve the sediment deposition changes for this specific period, other varve records
511 from the Arctic have also captured these warmer decades through greater sediment
512 deposition (e.g. Lake A and Sawtooth Lake, Fig. 9).

513 The winter climate signal recorded in the varves of Chevalier Bay appears to be
514 representative for a large part of the western Canadian Arctic Archipelago (Fig. 8).
515 However, our past winter reconstruction remains difficult to validate due to a lack of
516 quantitative winter temperature records available for comparison (e.g. McKay and
517 Kaufmann, 2014). The solution presented in this study came from the comparison with
518 annual temperature records and winter-weighted proxies (Fig. 8a). Long-term
519 similarities are evident between our winter temperature reconstruction and: (i) annual
520 temperature anomaly north of 60°N for the period CE 1900 - 2003 (ACIA 2004); (ii)
521 annual mass balance from the Melville Ice Cap for CE 1960 - 2010 (Boon et al. 2010);
522 and (iii) annual temperature record ($\delta^{18}\text{O}$) from the Devon Ice Cap extending towards
523 CE 1973 (Fisher et al. 1983). The correlation map between winter and annual
524 temperature during the instrumental period supports these similarities among the
525 records ($r= 0.4$, $n= 385$), with spatial correlations up to $r= 0.5$ (Fig. 8c). The similarity of
526 our winter reconstruction to observed and inferred annual temperatures suggests that
527 the Chevalier Bay record contains a more regional signal. But more importantly,
528 differences between the two records (>75 % unexplained variance) underline the
529 potential of the winter reconstruction. Indeed, this study highlights the need to consider
530 the winter season in climate syntheses and in climate models in order to reduce

531 uncertainty in sensitivity tests of the Earth's climate to natural and anthropogenic
532 forcings.

533 The comparison with other published varve records highlights the challenge of deriving
534 a common picture for the winter season using Arctic lake sediments (Fig. 9). While intra-
535 seasonal and geographical climate differences still exist, Arctic lakes with similar nival
536 properties are all very sensitive to specific sedimentation processes. Well-dated varve
537 records from Arctic lakes have previously been used to reconstruct: (i) spring discharge,
538 indirectly through catchment snow water equivalent (Lamoureux et al. 2006); (ii)
539 autumn temperature and snowfall (Tomkins et al. 2010); (iii) the intensity of the spring
540 snowmelt through median particle-size measured for each varve (Francus et al. 2002);
541 (iv) the maximum snow accumulation prior the first-above 0°C spring temperature
542 (Cuven et al. 2011); or (v) more regional melt season temperatures (Cook et al. 2008).
543 These catchment-specific sedimentation processes and responses led to reconstructed
544 climate records that are substantially different, at both annual and multi-decadal time
545 scales (Fig. 9). This raises important concerns regarding the influence of the size, and the
546 topography of the catchment on the sedimentation, even for lakes that have comparable
547 hydroclimatic and geologic properties. Furthermore, the differences among the varve
548 records underline the importance of understanding sedimentation processes and for
549 climate sensitivity tests from each individual site prior to reconstruct past climate from
550 the Arctic.

551 The range of climatic signals interpreted from High Arctic varve records is diverse
552 (Figure 10). The quantitative record for the extended winter from Chevalier Bay offers a
553 unique opportunity to evaluate climate change in the Arctic. Although this nival
554 catchment appears to respond to the length and the intensity of snowmelt, the indirect
555 information stored in the winter temperature and winter snowfall conditions holds a
556 greater potential. This record could be used in more applied climate research such as
557 data-model comparisons and proxy-data assimilation in climate model simulations over
558 the past c. 400 years (Goosse et al. 2010).

559 **6 Summary and conclusions**

560

561 We have investigated the varved sediments of Chevalier Bay with the aim to increase the
562 paleoclimate data coverage for winter; the most sensitive season to climate change in
563 the Arctic. We produced a well-calibrated quantitative temperature record for the
564 'extended' winter season (NDJFM) to CE 1670, which is representative of a large part of
565 the western Canadian High Arctic.

566 Based on detailed facies analysis of the relatively thick varves of Chevalier Bay, we
567 isolated and separated the nival units (spring snowmelt) from the rainfall units
568 (summer), and from clay caps (winter). This distinction was a basis for the development
569 of a reliable chronology and a good proxy-climate calibration model. Supported by an
570 accurate varve chronology, we demonstrate that the thickness of the nival units can be
571 used as a good predictor for winter climate conditions in this region of the Arctic. We
572 develop a proxy-climate calibration model to predict NDJFM temperature ($r= 0.71$, $p_c <$
573 0.01), while significant correlations are also found for NDJFM snowfall ($r= 0.65$, $p_c <$
574 0.01). This validates our working hypothesis in which the thickness of the nival units is
575 directly controlled by SWE and spring snowmelt, and ultimately by winter temperature
576 and related snowfall conditions. These results are significant and consistent among all
577 climate datasets considered for this study (Mould Bay, Resolute Bay, and gridded CRU
578 TS), and in agreement with neighbouring sedimentary process studies.

579 Our ~400-year long reconstruction compares well with annual temperature records for
580 this part of the Arctic, both on decadal and centennial time scales. This clearly suggests a
581 more regional climate signal, while important differences between the annual and
582 winter records underline the importance in considering and separating the winter
583 season in paleoclimate syntheses. On the contrary, the comparison of winter records
584 from lake sediment studies reveals a strong sensitivity to local climate change with site-
585 specific responses within each catchment. This gives additional interest for the extended
586 winter-season reconstruction from Chevalier Bay.

587 Our reconstruction reports the highest rate of warming ($0.37^\circ\text{C}/\text{decade}$) starting in the
588 late 1960s. This value is in agreement with the $0.40^\circ\text{C}/\text{decade}$ for annual means
589 reported for the Arctic over the period CE 1960-2003 (ACIA, 2004). Projected increases
590 in winter temperature together with increased snowfall are expected to have prominent

591 effects on the Arctic environment such as for instance: (i) greater permafrost thaw depth,
592 and the alteration in annual carbon balance of northern-latitude ecosystems, towards
593 greater loss of CO₂ to the atmosphere (Natali et al., 2014); (ii) the alteration in the
594 tundra biosphere-atmosphere interactions (Morgado et al. 2016); and (iii) the
595 acceleration of sea-ice retreat resulting in a greater proportion of Arctic surface
596 evaporative change (Bitanja and Selten, 2014). All these effects contribute to a positive
597 feedback to climate change towards higher winter temperatures in the Arctic.

598

599

600 **Acknowledgments**

601

602 This research was carried out within the Swiss National Science Foundation grant
603 P2BEP2_162029, and supported by NSERC/CRSNS 2015-05276. We thank K. Kathan and
604 E. Kjikjerkovska for their early contributions to research on Chevalier Bay. Thanks to A.
605 Normandeau, J. Fouché, G. King, and A. Rudy for fruitful discussions. Particular thanks
606 also go to the PEARL Lab of J. Smol for access to the gamma counter, and to C. Grooms
607 and B. Sivarajah for their help with sample preparation and dating. We would also like to
608 acknowledge Polar Continental Shelf Program, Natural Resources Canada for field
609 logistics support. Constructive comments from two anonymous reviewers are
610 appreciated.

611 **Figure captions**

612 **Fig. 1** Study site with: **A** location of Chevalier Bay, Melville Island in the Canadian High
 613 Arctic. Orange squares indicate meteorological stations, while the small dashed area
 614 shows the grid cell region used from CRU TS 3.23, **B** catchment properties of Lake
 615 Chevalier and its hydrology, **C** averaged meteorological data for the period CE 1949 –
 616 1997 obtained from the station of Mould Bay A.

617 **Fig. 2** Water column properties of Chevalier Bay on June 20, 2010: salinity (PSU),
 618 turbidity (NTU), temperature (°C) and dissolved oxygen (%).

619 **Fig. 3** Sediment properties with: **A** core image and XRF scans, **B** example of varve years
 620 and their associated XRF characteristics. N refers to the nival unit, R for the rainfall unit
 621 and Cc to clay cap.

622 **Fig. 4** Varve facies types occurring in the sedimentary sequence of Chevalier Bay. N
 623 stands for the nival unit, R for the rainfall unit, Cc for clay cap, Cci for the intermediate
 624 clay cap, and Sp for slump.

625 **Fig. 5** Varve chronology obtained from thin section measurements. Counting uncertainty
 626 (error) is reported by the shaded area around the final age-depth line (visual), and by
 627 the dashed line on the lower panel (quantitative values).

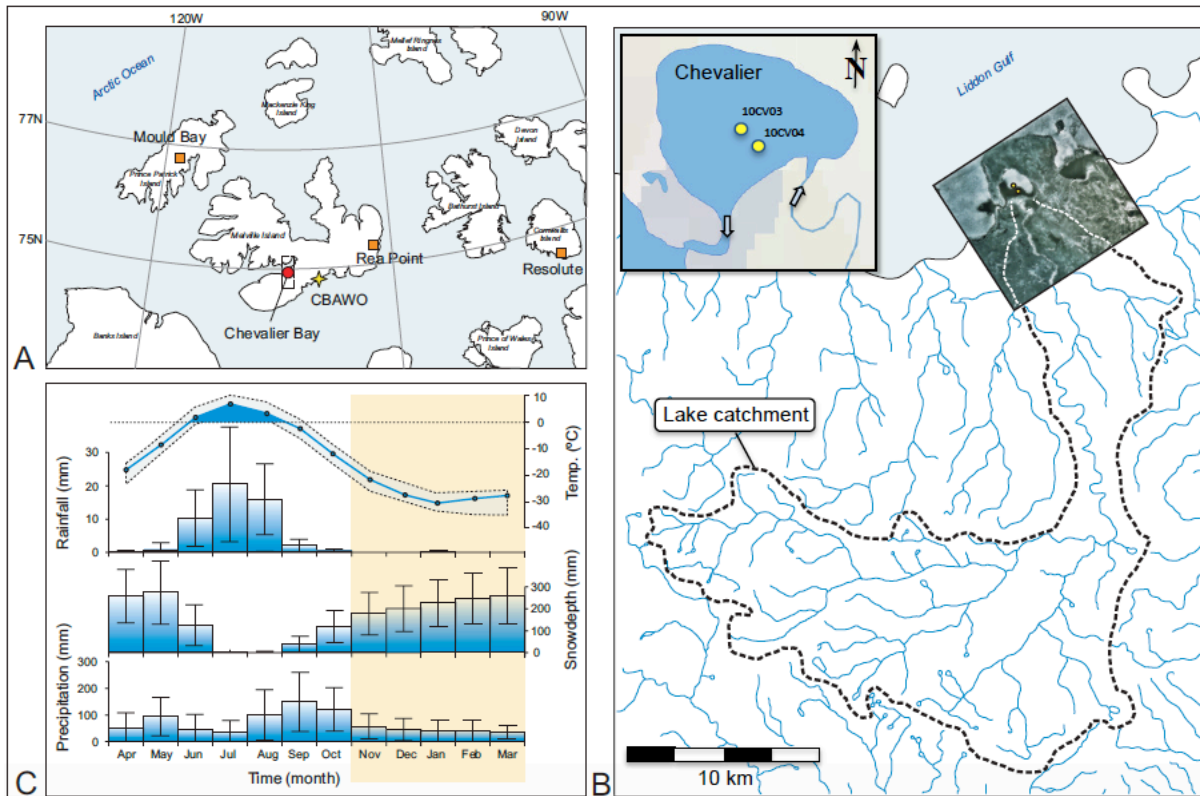
628 **Fig. 6** Principal component analysis (PCA) integrating the thickness of the nival units
 629 (indicated as 'varve'), and monthly climate data obtained from Mould Bay (Mould),
 630 Resolute Bay (Res.) and the CRU TS grid cell (CRU). The four seasons (MAM, JJA, SON,
 631 DJF) and specific seasons of interest (ASO and NDJFM) are considered here.

632 **Fig. 7 A** Linear correlations between the different meteorological datasets considered in
 633 this study, **B** time series of NDJFM temperature from each station combined with the
 634 calibration-in-time model obtained from the thickness of the nival units in Chevalier Bay.

635 **Fig. 8 A** Comparison between the winter NDJFM temperature records from Chevalier
 636 Bay and the annual temperature records from the Arctic North 60°N (ACIA, 2004), the
 637 ice core $\delta^{18}\text{O}$ record from the Devon Ice Cap (Fisher et al. 1983) and the annual mass
 638 balance of the South Melville Ice Cap (Boon et al. 2010). Note that the black line (our
 639 study) and the blue line (Fisher et al. 1983) positively correlate with $r=0.37$ ($p < 0.01$, $n =$
 640 385), **B** correlation maps of NDJFM temperature for the Canadian High Arctic, **C**
 641 correlation maps between NDJFM temperature at our study site and annual temperature
 642 for the rest of the Arctic (for the period CE 1949-1997).

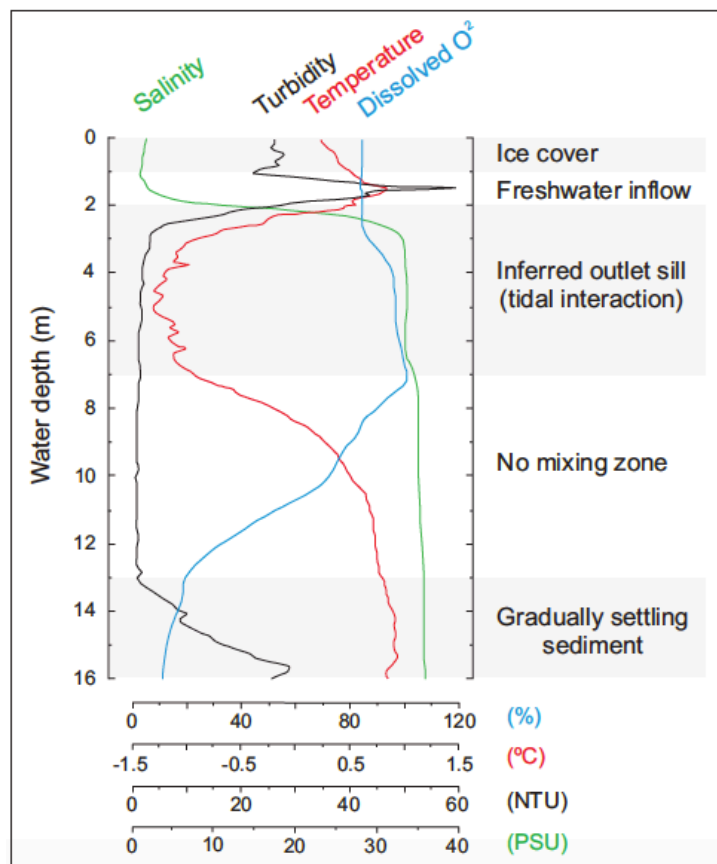
643 **Fig. 9** Comparison between the different winter-sensitive varved sediment records
 644 published from the Canadian High Arctic with their respective location. Data are shown
 645 with an 11-year triangular filter.

646 **Fig. 10** Illustration of the different correlations between sediment proxy data (mostly
 647 varve thickness) and monthly climate variables from nival-catchment lake records
 648 located in the Canadian High Arctic. Results are from Sanagak Lake (Lamoureux et al.
 649 2006), Lake A (Tomkins et al. 2010), Sawtooth Lake (Francus et al. 2002), East Lake
 650 (Cuven et al. 2011), and Lower Lake Murray (Cook et al. 2008). Asterisks are for records
 651 that depend on the year-to-year timing of the melting. The thick dark line shows
 652 Chevalier Bay record (winter NDJFM temperature, this study).



653
654
655

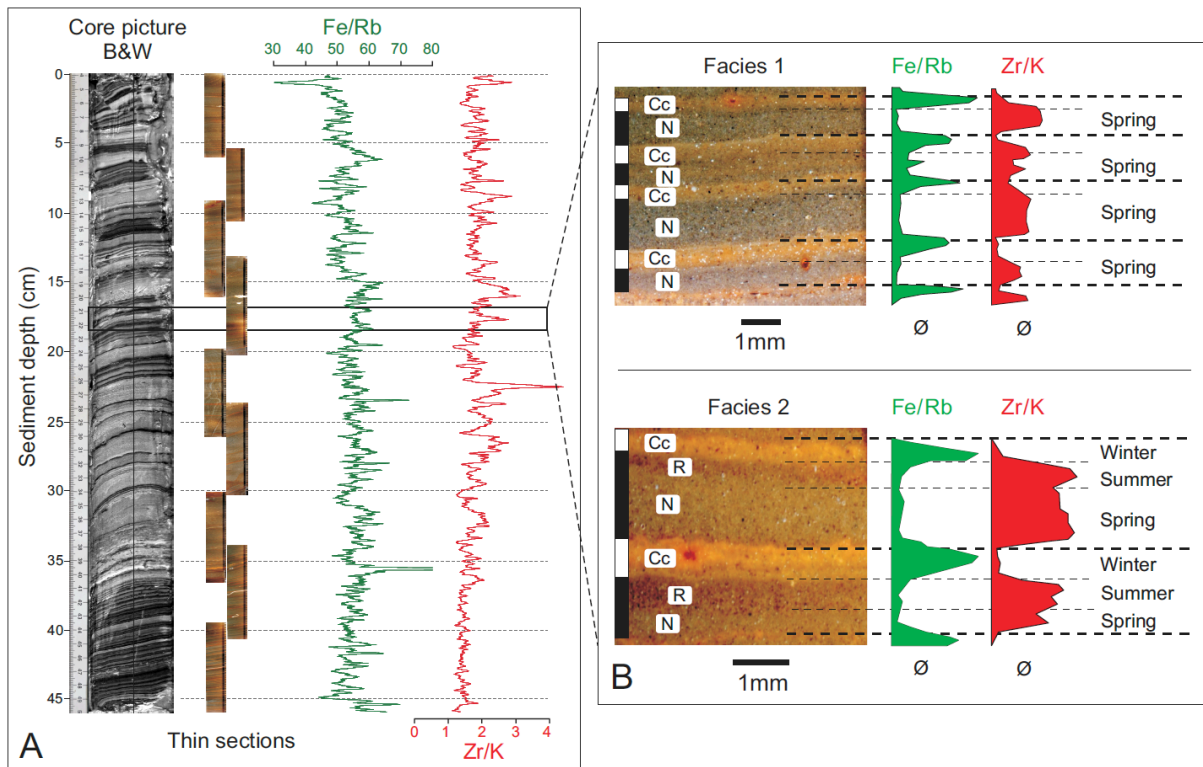
Fig. 1



656
657

Fig. 2

658

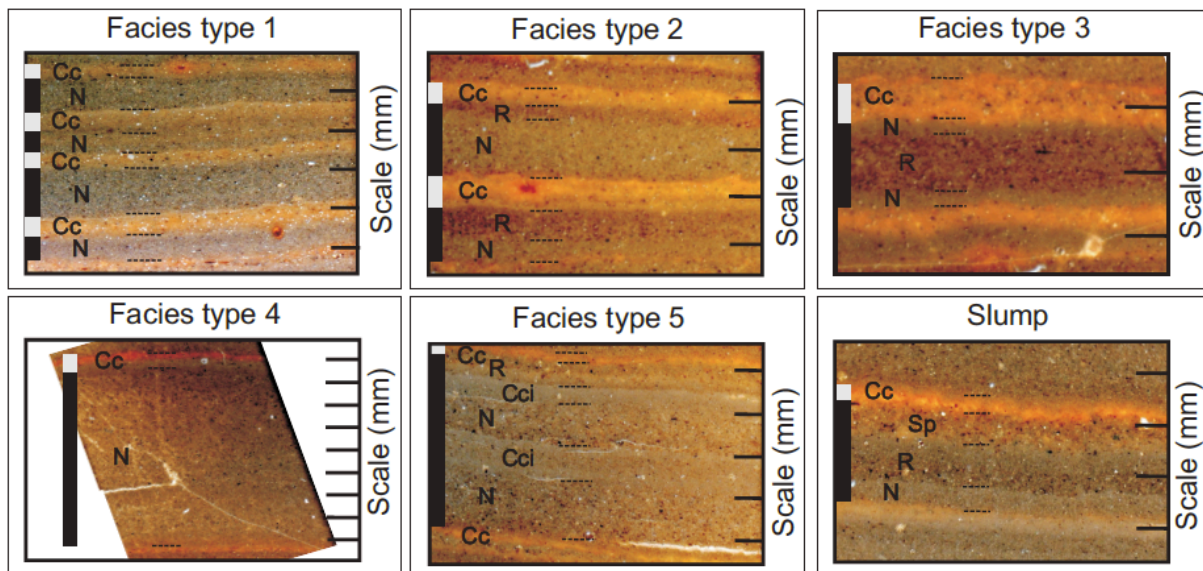


659

660

661

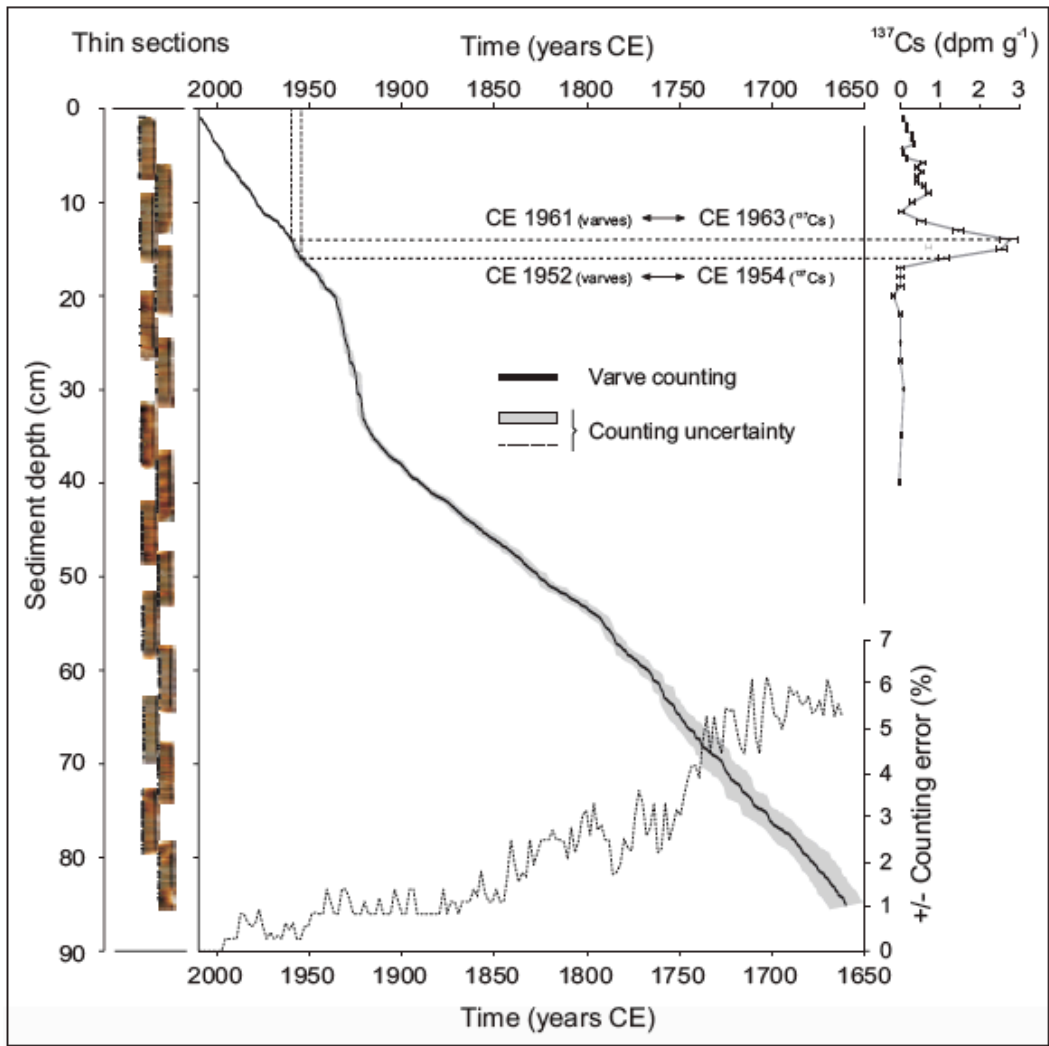
Fig. 3



662

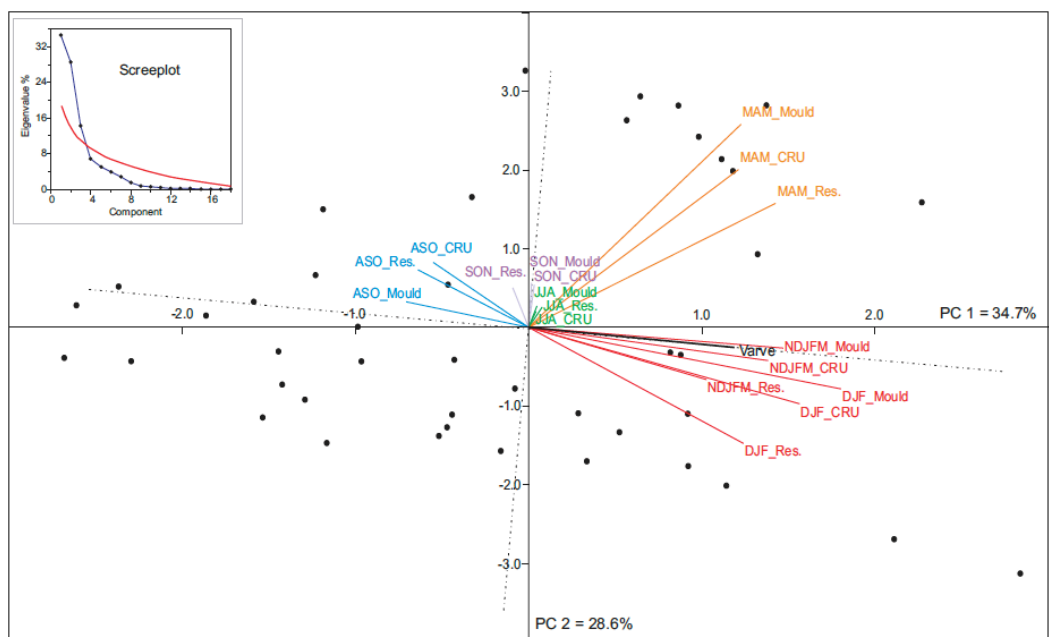
663

Fig. 4



664
665
666
667

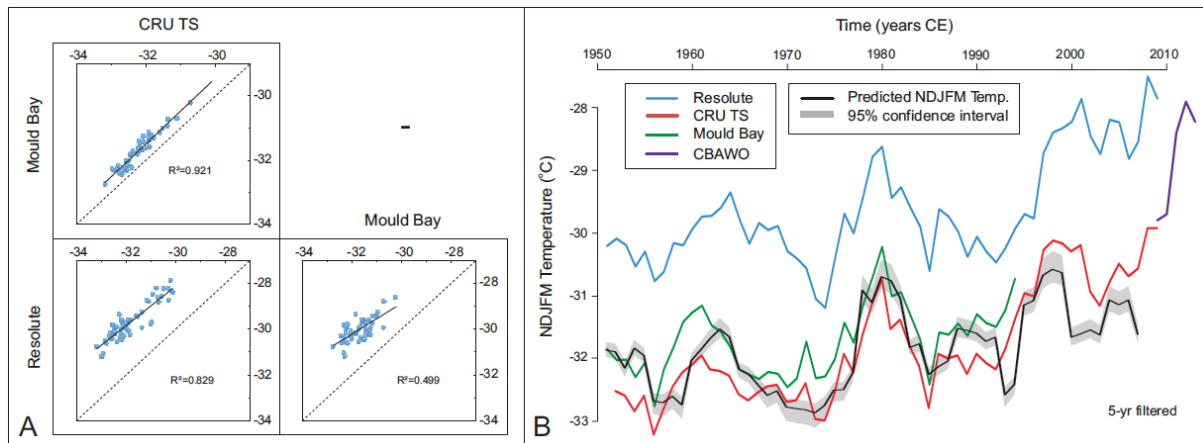
Fig. 5



668

669 **Fig. 6**

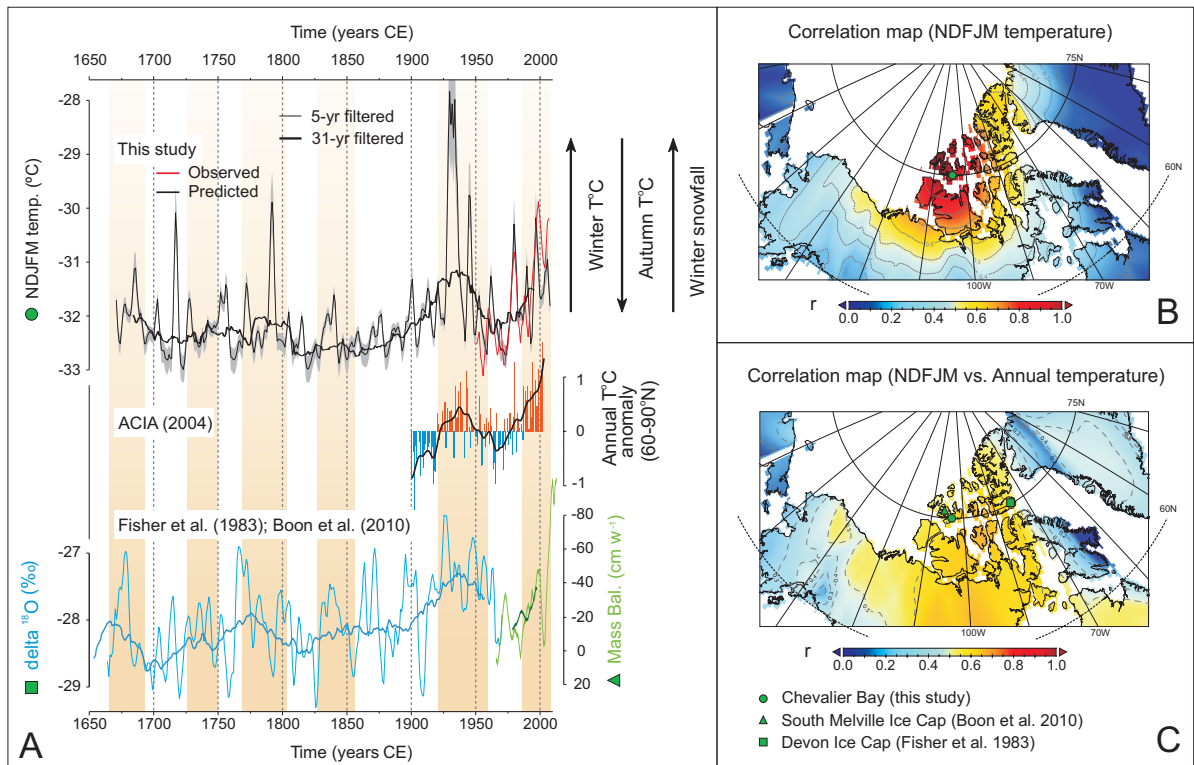
670



671

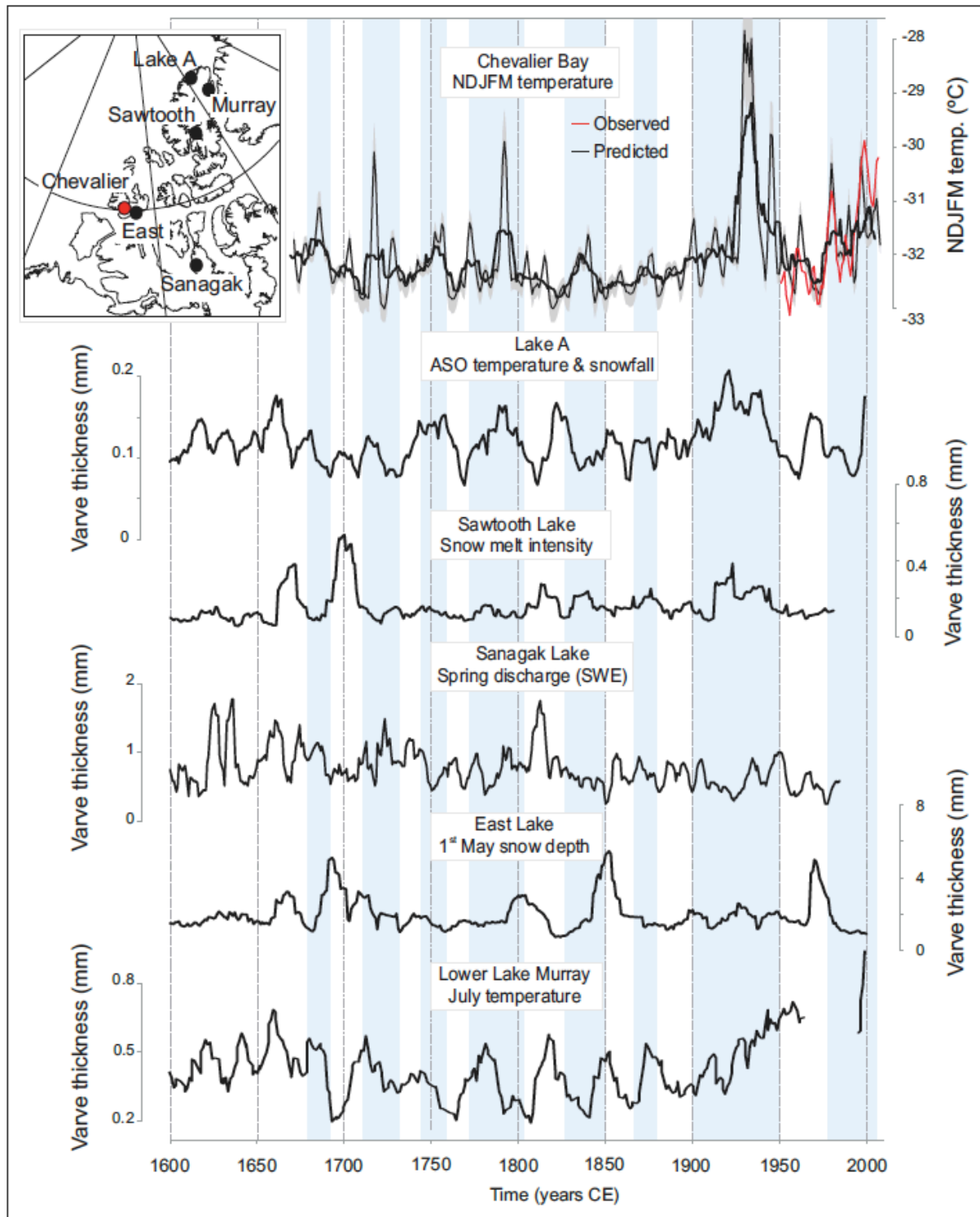
672 **Fig. 7**

673



674

675 **Fig. 8**

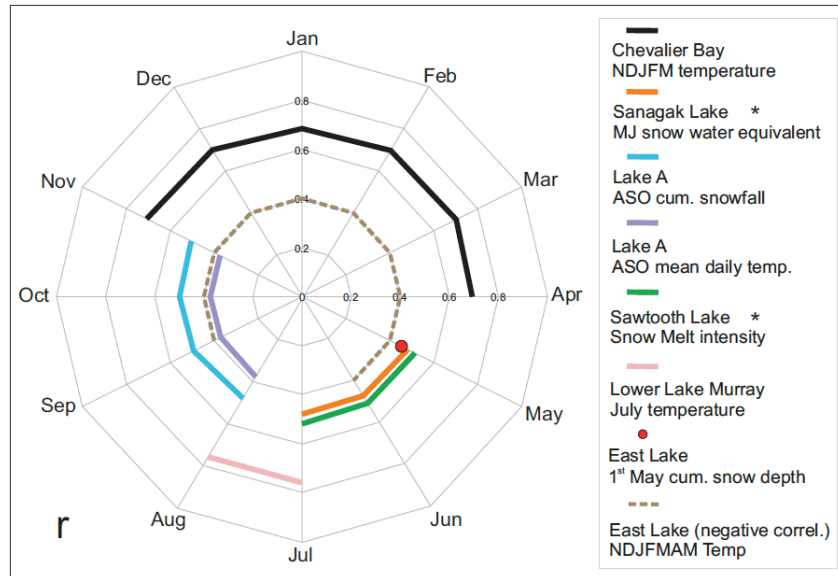


676

677

678

Fig. 9



679
680 **Fig. 10**

681
682
683

684 **Table 1** Correlation table between the thickness of the varve nival units and climate
685 data from Mould Bay, Resolute Bay and CRU TS 3.23. Highest correlation results from
686 multiple testing are reported for temperature, precipitation and snowfall
687

Temp.	Mould Bay			Resolute			CRU TS		
	r_0	r_3	r_5	r_0	r_3	r_5	r_0	r_3	r_5
JF	0.44**	0.51**	0.60**	0.07	0.21	0.35	0.36	0.58	0.71
NDJFM	0.32	0.48**	0.66**	0.27*	0.49**	0.65**	0.27*	0.45*	0.71**
NDJFMAM	0.34*	0.44**	0.55**	0.26*	0.51**	0.67**	0.26*	0.43*	0.68**
ASO	-0.11	-0.49**	-0.52*	-0.15	-0.20	-0.10	-0.14	-0.33	-0.34
Precip.									
NDJFM	0.22	0.24	0.21	0.12	0.47*	0.57**	0.27*	0.45**	0.61**
Snowfall									
NDJFM	0.16	0.23	0.26	0.14	0.53**	0.63**	0.27*	0.45*	0.61**

* $p_c < 0.05$

** $p_c < 0.01$

688

689 **References**

690

691 1. ACIA, 2004. Impacts of a Warming Arctic: Arctic Climate Impact Assessment.
692 Cambridge University Press, pp 1-1020

693 2. Amann B., Szidat S., Grosjean M., 2015. A millennial-long record of warm season
694 precipitation and flood frequency for the North-western Alps inferred from varved lake
695 sediments: implications for the future. *Quat Sci Rev* 115: 89-100

696 3. Bengtsson L., Semenov V. A., Johannessen O. M., 2004. The Early Twentieth-Century
697 Warming in the Arctic—A Possible Mechanism. *Amer Meteorol Soc* 17: 4045-4057_Doi:
698 10.1175/1520-0442(2004)017<4045:TETWIT>2.0.CO;2

699 4. Besonen M. R., Patridge W., Bradley R. S., Francus P., Stoner J. S., Abbot M. B., 2008. A
700 record of climate over the last millennium based on varved lake sediments from the
701 Canadian High Arctic. *Holocene* 18: 169-180_Doi: 10.1177/0959683607085607

702 5. Bintanja R., Selten F. M., 2014. Future increases in Arctic precipitation linked to local
703 evaporation and sea-ice retreat. *Nature* 509: 479-482_Doi:10.1038/nature13259

704 6. Birks H. J. B., 2005. Overview of numerical methods in palaeolimnology. In: Birks H. J.
705 B., Lotter A. F., Juggins S. (eds) *Tracking environmental change using lake sediments:*
706 *data handling and numerical techniques.* Kluwer, Dordrecht, pp 19–92

707 7. Braun C., Hardy D. R., Bradley R. S., 2000. Streamflow and suspended sediment
708 transfer to Lake Sophia, Cornwallis Island, Nunavut, Canada. *Arct Antarct Alp Res* 32:
709 456-465_Doi: 10.2307/1552395

710 8. Briner J. P., McKay N. P., Axford Y., Bennike O., Bradley R. S., de Vernal A., Fisher D.,
711 Francus P., Fréchette B., Gajewski K., Jennings A., Kaufman D. S., Miller G., Rouston C.,
712 Wagner B., 2016. Holocene climate change in Arctic Canada and Greenland. *Quat Sci Rev*
713 1-15_10.1016/j.quascirev.2016.02.010

714 9. Boon S., Burgess D. O., Koerner R. M., Sharp M. J., 2010. Forty-seven Years of Research
715 on the Devon Island Ice Cap, Arctic Canada. *Arctic* 63: 13-29_Doi: 10.14430/arctic643

716 10. Christie R. L., McMillan N. J., 1994. The geology of Melville Island, Arctic Canada. *Geol*
717 *Surv Can bulletin* 450_ISBN 0-660-14982-6

718 11. Chutko K. J., Lamoureux S. F., 2008. Identification of coherent links between
719 interannual sedimentary structures and daily meteorological observations in Arctic
720 proglacial lacustrine varves: potentials and limitations. *Can J Earth Sci* 45: 1-13_Doi:
721 10.1139/E07-070

722 12. Cockburn J. M. H., Lamoureux S. F., 2008. Hydroclimate controls over seasonal
723 sediment yield in two adjacent High Arctic watersheds. *Hydrol Process* 22: 2013-
724 2027_Doi: 10.1002/hyp.6798

725 13. Coey J. M. D., Schindler D. W., Weber F., 1974. Iron compounds in lake sediments. *Can*
726 *J Earth Sci* 11: 1489-1493_Doi: 10.1139/e74-142

727 14. Collins, M., R. Knutti, J. Arblaster, J.-L. Dufresne, T. Fichet, P. Friedlingstein, X. Gao,
728 W.J. Gutowski, T. Johns, G. Krinner, M. Shongwe, C. Tebaldi, A.J. Weaver and M. Wehner,
729 2013: Long-term Climate Change: Projections, Commitments and Irreversibility. In:
730 *Climate Change 2013: The Physical Science Basis. Contribution of Working Group I to*
731 *the Fifth Assessment Report of the Intergovernmental Panel on Climate Change* [Stocker,

- 732 T.F., D. Qin, G.-K. Plattner, M. Tignor, S.K. Allen, J. Boschung, A. Nauels, Y. Xia, V. Bex and
733 P.M. Midgley (eds.)). Cambridge University Press, Cambridge, United Kingdom and New
734 York, NY, USA
- 735 15. Comiso J. C., Hall D. K., 2014. Climate trends in the Arctic as observed from space.
736 WIREs Clim Change 5: 389-409_DOI: 10.1002/wcc.277
- 737 16. Cook T. L., Bradley R. S., Stoner J. S., Francus P., 2008. Five thousand years of
738 sediment transfer in a high arctic watershed recorded in annually laminated sediments
739 from Lower Murray Lake, Ellesmere Island, Nunavut, Canada. J Paleolimnol 44: 77-
740 94_DOI: 10.1007/s10933-008-9252-0
- 741 17. Croudace I. W., Rindby A., Rothwell R. G., 2006. ITRAX: description and evaluation of
742 a new sediment core scanner. In: Rothwell R. G., (ed). New techniques in sediment core
743 analysis. Geol Soc London, 267: 51-63_DOI: 10.1144/GSL.SP.2006.267.01.04
- 744 18. Cuven S., Francus P., Lamoureux S. F., 2010. Estimation of grain size variability with
745 micro X-ray fluorescence in laminated lacustrine sediments, Cape Bounty, Canadian High
746 Arctic. J Paleolimnol 44: 803-817_DOI: 10.1007/s10933-010-9453-1
- 747 19. Cuven S., Francus P., Lamoureux S., 2011. Mid to Late Holocene hydroclimatic and
748 geochemical records from the varved sediments of East Lake, Cape Bounty, Canadian
749 High Arctic. Quat Sci Rev 30: 2651-2665_DOI: 10.1016/j.quascirev.2011.05.019
- 750 20. de Jong R., Kamenik C., 2011. Validation of a chrysophyte stomatocyst-based cold-
751 season climate reconstruction from high Alpine Lake Silvaplana, Switzerland. J Quat Sci
752 26: 268-275_DOI: 10.1002/jqs.1451
- 753 21. Favaro E. A., Lamoureux S. F., 2014. Antecedent controls on rainfall runoff response
754 and sediment transport in a High Arctic Catchment. Geografiska Annaler A, Phys Geog
755 96: 433-446_DOI: 10.1111/geoa.12063
- 756 22. Fisher D. A., Koerner R. M., Paterson W. S. B., Dansgaard W., Gundestrup N., Reeh N.,
757 1983. Effect of wind scouring on climatic records from ice-core oxygen-isotope profiles.
758 Nature 301: 205-209_DOI: 10.1038/301205a0
- 759 23. Forbes A. C., Lamoureux S. F., 2005. Climatic Controls on Streamflow and Suspended
760 Sediment Transport in Three Large Middle Arctic Catchments, Boothia Peninsula,
761 Nunavut, Canada. Arct Antarct Alp Res 37: 304-315_DOI: 4095891
- 762 24. Francus P., Bradley R. S., Abbott M. B., Patridge W., Keimig F., 2002. Paleoclimate
763 studies of minerogenic sediments using annually resolved textural parameters. Geophys
764 Res Lett 29: 1-4_DOI: 10.1029/2002GL015082
- 765 25. Francus P., Bradley R. S., Lewis T., Abbott M., Retelle M., Stoner J. S., 2008.
766 Limnological and sedimentary processes at Sawtooth Lake, Canadian High Arctic, and
767 their influence on varve formation. J Paleolimnol 40: 963-985_DOI: 10.1007/s10933-
768 008-9210-x
- 769 26. Goose H., Crespin E., de Montety A., Mann M. E., Renssen H., Timmermann A., 2010.
770 Reconstructing surface temperature changes over the past 600 years using climate
771 model simulations with data assimilation. J Geophys Res 115: D09108_DOI:
772 10.1029/2009JD012737
- 773 27. Haese R. R., 2006. The reactivity of iron. In: Schultz H. D., Zabel M. (eds). Springer,
774 Berlin Heidelberg, pp 233-261_DOI: 10.1007/978-3-662-04242-7_7

- 775 28. Hall, A., 2004. The role of surface albedo feedback in climate. *J Clim* 17: 1550-1568_
776 DOI: 10.1175/1520-0442(2004)017<1550:TROSAF>2.0.CO;2
- 777 29. Hambley, G. W., Lamoureaux, S. F., 2006. Recent summer climate recorded in complex
778 varved sediments, Nicolay Lake, Cornwall Island, Nunavut, Canada. *J Paleolimnol* 35:
779 629-640_DOI: 10.1007/s10933-005-4302-3
- 780 30. Hardy D. R., Bradley R. S., Zolitschka B., 1996. The climatic signal in varved sediments
781 from Lake C2, northern Ellesmere Island, Canada. *J Paleolimnol* 16: 227-238_DOI:
782 10.1007/BF00176938
- 783 31. Harris I., Osborn T. J., Lister D. H., 2014. Updated high-resolution grids of monthly
784 climatic observations – the CRU TS3.10 Dataset. *Int J Climatol* 34: 623-642_DOI:
785 10.1002/joc.3711
- 786 32. Hodgson D. A., Vincent J. S., and Fyles J. G., 1984. Quaternary geology of central
787 Melville Island, Northwest Territories. *Geol Surv Can* 83, pp32_DOI: 10.4095/119784
- 788 33. Holmgren S. U., Bigler C., Ingólfsson Ó., Wolfe A. P., The Holocene–Anthropocene
789 transition in lakes of western Spitsbergen, Svalbard (Norwegian High Arctic): climate
790 change and nitrogen deposition. *J Paleolimnol* 43: 393-412_DOI: 10.1007/s10933-009-
791 9338-3
- 792 34. Hormes A., Bakke J., 2014. The quest for temperature and hydroclimate records.
793 *Arctic2k Working Group special issue. PAGES Magazine*
- 794 35. Hormes, A., Werner J., Husum K., Steiger N. J., 2015 Spatiotemporal distribution of
795 temperature and hydroclimate proxy data in the Arctic. *Arctic2k Working Group special*
796 *issue. Workshop report Arctic2k meeting, Vienna, Austria*
- 797 36. Hughen K. A., Overpeck J. T., Anderson R. F., Williams K. M., 1996. The potential of
798 palaeoclimate records from varved Arctic lake sediments: Baffin Island, Eastern
799 Canadian Arctic. In: Kemp, A. E. S. (eds). *Palaeoclimatology and Palaeoceanography from*
800 *Laminated Sediments, Geological Society Special Publication 116: 57-71_ ISBN 1-*
801 *897799-67-5*
- 802 37. Hughen K. A., Overpeck J. T., Anderson R. F., 2000. Recent warming in a 500-year
803 palaeotemperature record from varved sediments, Upper Soper Lake, Baffin Island,
804 Canada. *Holocene* 10: 9-19_DOI: 10.1191/095968300676746202
- 805 38. Johannessen O. M., Kuzmina S. I., Bobylev L. P., Miles M. W., 2016. Surface air
806 temperature variability and trends in the Arctic: new amplification assessment and
807 regionalisation. *Tellus A* 68: 28234_DOI: 10.3402/tellusa.v68.28234
- 808 39. Jones P. D., Harpham C., Vinther B. M., 2014. Winter-responding proxy temperature
809 reconstructions and the North Atlantic Oscillation, *J Geophys Res Atmos* 119: 6497-
810 6505_DOI:10.1002/2014JD021561
- 811 40. Kattsov V. M., Walsh J. E., 2000. Twentieth-century trends of Arctic precipitation
812 from observational data and a climate model simulation. *J Clim* 13: 1362-1370_DOI:
813 10.1175/1520-0442(2000)013<1362:TCTOAP>2.0.CO;2
- 814 41. Kattsov V. M., Walsh J. E., Chapman W. L., Govorkova V. A., Pavlova T. V., Zhang X.,
815 2007. Simulation and projection of Arctic freshwater budget components by the IPCC
816 AR4 global climate models. *J Hydrometeor* 8: 571-589_doi:10.1175/JHM575.1

- 817 42. Kaufman D. S., 2009. An overview of late Holocene climate and environmental
818 change inferred from Arctic lake sediment. *J Paleolimnol* 41: 1-6_DOI: 10.1007/s10933-
819 008-9259-6
- 820 43. Kurita N., 2011. Origin of Arctic water vapor during the ice-growth season. *Geophys*
821 *Res Lett* 38: L02709_DOI: 10.1029/2010GL046064
- 822 44. Kylander M. E., Ampel L., Wohlfarth B., Veres D., 2011. High-resolution X-ray
823 fluorescence core scanning analysis of Les Echets (France) sedimentary sequence: new
824 insights from chemical proxies. *J Quat Sci* 26: 109-117_DOI: 10.1002/jqs.1438
- 825 45. Lafrenière M. J., Laurin E., Lamoureux S. F., 2013. The impact of snow accumulation
826 on the active layer thermal regime in High Arctic soils. *Vadose Zone J.* DOI:
827 10.2136/vzj2012.0058
- 828 46. Lamoureux S. F., 1994. Embedding unfrozen lake sediments for thin section
829 preparation. *J Paleolimnol* 10: 141-146_DOI: 10.1007/BF00682510
- 830 47. Lamoureux S. F., 1999. Spatial and interannual variations in sedimentation patterns
831 recorded in nonglacial varved sediments from the Canadian High Arctic. *J Paleolimnol*
832 21: 73-84_DOI: 10.1023/A:1008064315316
- 833 48. Lamoureux S. F., 2000. Five centuries of interannual sediment yield and rainfall-
834 induced erosion in the Canadian High Arctic recorded in lacustrine varves. *Water Resour*
835 *Res* 36: 309-318_DOI: 10.1029/1999WR900271
- 836 49. Lamoureux S. F., Gilbert R., Lewis T., 2002. Lacustrine sedimentary environments in
837 High Arctic Proglacial Bear Lake, Devon Island, Nunavut, Canada. *Arct Antarct Alp Res*
838 34: 130-141_DOI: 10.2307/1552464
- 839 50. Lamoureux S. F., Gilbert R., 2004. A 750-yr record of autumn snowfall and
840 temperature variability and winter storminess recorded in the varved sediments of Bear
841 Lake, Devon Island, Arctic Canada. *Quat Res* 61: 134-147_
842 DOI:10.1016/j.yqres.2003.11.003
- 843 51. Lamoureux S. F., Stewart K. A., Forbes A. C., Fortin D., 2006. Multidecadal variations
844 and decline in spring discharge in the Canadian middle Arctic since 1550 AD. *Geophys*
845 *Res Lett* 33: L02403_DOI: 10.1029/2005GL024942
- 846 52. Lapointe F., Francus P., Lamoureux S. F., Saïd M., Cuvén S., 2012. 1750 years of large
847 rainfall events inferred from particle size at East Lake, Cape Bounty, Melville Island,
848 Canada. *J Paleolimnol* 48: 159-173_DOI:10.1007/s10933-012-9611-8
- 849 53. Lewis T., Lafrenière M. J., Lamoureux S. F., 2012. Hydrochemical and sedimentary
850 responses of paired High Arctic watersheds to unusual climate and permafrost
851 disturbance, Cape Bounty, Melville Island, Canada. *Hydrol Process* 26: 2003-2008_ DOI:
852 10.1002/hyp.8335
- 853 54. Masson-Delmotte V., Schulz M., Abe-Ouchi A., Beer J., Ganopolski A., González Rouco J.
854 F., Jansen E., Lambeck K., Luterbacher J., Naish T., Osborn T., Otto-Bliesner B., Quinn T.,
855 Ramesh R., Rojas M., Shao X., Timmermann A., 2013. Information from Paleoclimate
856 Archives. In: *Climate Change 2013: The Physical Science Basis. Contribution of Working*
857 *Group I to the Fifth Assessment Report of the Intergovernmental Panel on Climate*
858 *Change* [Stocker T. F., Qin D., Plattner G. -K., Tignor M., Allen S. K., Boschung J., Nauels A.,
859 Xia Y., Bex V. and Midgley P. M. (eds.)]. Cambridge University Press, Cambridge, United
860 Kingdom and New York, NY, USA

- 861 55. McKay N. P., Kaufman D. S., 2014. An extended Arctic proxy temperature database
862 for the past 2,000 years. *Sci Data* 1: 140026_DOI: 10.1038/sdata.2014.26
- 863 56. Miller G. H., Alley R. B., Brigham-Grette J., Fitzpatrick J. J., Polyak L., Serreze M., White
864 J. W. C., 2010. Arctic Amplification: can the past constrain the future? *Quat Sci Rev* 29:
865 1779-1790_DOI: 10.1016/j.quascirev.2010.02.008
- 866 57. Morgado L. N., Semenova T. A., Welker J. M., Walker M. D., Smets E., Geml J., 2016.
867 Long-term increase in snow depth leads to compositional changes in arctic
868 ectomycorrhizal fungal communities. *Glo Cha Biol*_DOI: 10.1111/gcb.13294
- 869 58. Moritz R. E., Bitz C. M., Steig E. J., 2002. Dynamics of recent climate change in the
870 Arctic. *Science* 297: 1497-1502_DOI: 10.1126/science.1076522
- 871 59. Natali S. M., Schuur E. A. G., Webb E., Pries C. E. H., Crummer K. G., 2014. Permafrost
872 degradation stimulates carbon loss from experimentally warmed tundra. *Ecol* 95: 602-
873 608_DOI: 10.1890/13-0602.1
- 874 60. Overpeck J., Hughen K., Hardy D., Bradley R., Case R., Douglas M., Finney B., Gajewski
875 K., Jacoby G., Jennings A., Lamoureux S., Lasca A., MacDonald G., Moore J., Retelle M.,
876 Smith S., Wolfe A., Zielinski G., 1997. Arctic Environmental Change of the Last Four
877 Centuries. *Science* 278: 1251-1256_DOI: 10.1126/science.278.5341.1251
- 878 61. Rinke A., Dethloff K., Christensen J. H., 1999. Arctic winter climate and its interannual
879 variations simulated by a regional climate model. *J Geophys Res* 104: 19027-19038_DOI:
880 10.1029/1999JD900296
- 881 62. Smol J. P., Douglas M. S. V., 1996. From controversy to consensus: making the case for
882 recent climate change in the Arctic using lake sediments. *Front Ecol Environ* 5: 466-
883 474_DOI:10.1890/060162
- 884 63. Sundqvist, H. S, Kaufman D. S., McKay N. P., Balascio N. L., Briner J. P., Cwynar L. C.,
885 Sejrup H. P., Seppä H., Subetto D. A., Andrews J. T., Axford Y., Bakke J., Birks H. J. B.,
886 Brooks S. J., de Vernal A., Jennings A. E., Ljungqvist F. C., Rühland K. M., Saenger C., Smol J.
887 P., Viau A. E., 2014. Arctic Holocene proxy climate database—new approaches to
888 assessing geochronological accuracy and encoding climate variables. *Clim. Past Discuss*
889 10: 1-63_DOI:10.5194/cp-10-1605-2014
- 890 64. Thompson D. W. J., Wallace J. M., 1998. The Arctic Oscillation signature in the
891 wintertime geopotential height and temperature fields. *Geophys Res Lett* 25: 1297-
892 1300_DOI: 10.1029/98GL00950
- 893 65. Tomkins J. D., Lamoureux S. F., Antoniades D., Vincent W. F., 2010. Autumn snowfall
894 and hydroclimatic variability during the past millennium inferred from the varved
895 sediments of meromictic Lake A, northern Ellesmere Island, Canada. *Quat Res* 74: 188-
896 198_DOI: 10.1016/j.yqres.2010.06.005
- 897 66. von Gunten L., Grosjean M., Kamenik C., Fujak M., Urrutia R., 2012. Calibrating
898 biogeochemical and physical climate proxies from non-varved lake sediments with
899 meteorological data: methods and case studies. *J Paleolimnol* 47: 583-600_DOI:
900 10.1007/s10933-012-9582-9
- 901 67. Wolfe A. P., Miller G. H., Olsen C. A., Forman S. L., Doran P. T., 2004. Geochronology of
902 high latitude lake sediments. In: Pienitz R., Douglas M. S. V, Smol J.P. (eds). *Long-term*
903 *Environmental Change in Arctic and Antarctic Lakes*. Springer, Netherlands_ ISBN 978-
904 1-4020-2126-8

- 905 68. Wolf A. P., Smith I. R., 2004. Paleolimnology of the middle and High Canadian Arctic.
906 In: Pienitz R., Douglas M. S. V, Smol J.P. (eds). Long-term Environmental Change in Arctic
907 and Antarctic Lakes. Springer, Netherlands_ ISBN 978-1-4020-2126-8
- 908 69. Yamanouchi T., 2011. Early 20th century warming in the Arctic: A review. Polar Sci
909 5: 53-71_DOI: 10.1016/j.polar.2010.10.002